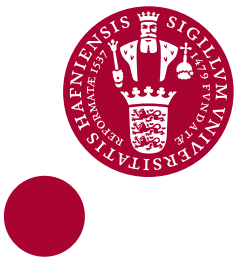

The stability of solitons in biomembranes and nerves

Lautrup, B.; Jackson, A.D.; Heimburg, Thomas Rainer

Published in:
arXiv.org: Physics

Publication date:
2005

Document version
Publisher's PDF, also known as Version of record

The stability of solitons in biomembranes and nerves

B. Lautrup, A. D. Jackson and T. Heimburg
Niels Bohr Institute, Blegdamsvej 17, DK-2100, Copenhagen Ø, Denmark
(Dated: February 2, 2008)

We examine the stability of a class of solitons, obtained from a generalization of the Boussinesq equation, which have been proposed to be relevant for pulse propagation in biomembranes and nerves. These solitons are found to be stable with respect to small amplitude fluctuations. They emerge naturally from non-solitonic initial excitations and are robust in the presence of dissipation.

PACS numbers: 80,87,87.10

INTRODUCTION

The action potential in nerves is a propagating voltage pulse across the axonal membrane with an amplitude of about 100 mV. In 1952, A. L. Hodgkin and A. F. Huxley proposed a theory for the nerve pulse which has since become the textbook model [1]. Their picture is based on the equilibration of ion gradients across the nerve membrane through specific ion-conducting proteins (called ion channels) which leads to transient voltage changes. Hodgkin-Huxley theory thus relies on dissipative processes and is intrinsically not isentropic. It is rather based on Kirchhoff circuits involing capacitors (the nerve membrane), resistors (the ion channels) and electrical currents introduced by the ion fluxes.

We have recently proposed an alternative model for the nerve pulses based on the propagation of a localized density pulse (soliton) in the axon membrane [2]. This model has several advantages over the Hodgkin-Huxley model. It explains the reversible temperature and heat changes observed in connection with the nerve pulse. (Such reversible changes are not consistent with the Hodgkin-Huxley theory but rather suggest that an isentropic process is responsible for the action potential [3, 4, 5].) It further predicts the correct pulse propagation velocities in myelinated nerves. These velocities are closely related to the lateral sound velocities in the nerve membrane. One essential feature of our model is the presence of empirically known lipid phase transitions slightly below physiological temperatures. The closer the phase transition is to physiological temperatures, the easier it is to excite the nerve pulse. Our model therefore immediately explains another interesting feature of nerve excitation, i.e., that the nerve pulse can be induced by a sudden cooling of the nerve, and that it can be inhibited by a temperature increase [7]. During compression, the appearance of a voltage pulse is merely a consequence of the piezo-electric nature of the nerve membrane, which is partially charged and asymmetric.

Another advantage of a soliton-based description of pulse propagation in nerves lies in its predictive power. Given measured values of the compression modulus as a function of lateral density and frequency, soliton properties (including its shape and its energy) can be determined uniquely as a function of soliton velocity. Given a measured soliton velocity, the theory contains no freely adjustable parameters and has the virtue of being falsifiable.

In [2] the possibility of soliton propagation was explored and compared to observations in real nerves. In the present paper we study some intrinsic features of these solitons, in particular the stability of such pulses in the presence of noise and dissipation. Such investigations are necessary to demonstrate that such pulses could propagate under realistic physiological conditions over the length scales of nerves (as much as several meters) even in the presence of friction and lateral heterogeneities. In the following section, we will state the model more precisely and derive the analytic form of its solitonic solutions. We will then turn to a description of the numerical methods used here. We use these methods to probe (i) the stability of solitons with respect to "infinitesimal" perturbations (i.e., lattice noise), (ii) the way in which solitons are produced by localized non-solitonic initial excitations of the system, and (iii) the behavior of solitons in the presence of dissipation. We will demonstrate that the solitons of Ref. [2] are remarkably robust with respect to all of these perturbations.

ANALYTIC CONSIDERATIONS

Thermodynamic measurements of the lipids of biological membranes reveal a number of interesting features of potential relevance for understanding the nature of pulses in biomembranes and nerves. In particular, such systems display an order-disorder transition at temperatures somewhat below that of biological interest from a low temperature "solid-ordered" phase to a high temperature "liquid-disordered" phase in which both the lateral order and chain order of the lipid molecules is lost [8]. The proximity of this phase transition to temperatures of biological interest has striking effects on the compression modulus and, hence, on the sound velocity [9, 10]. For densities some 10% above the equilibrium density, the low-frequency sound velocity is reduced by roughly a factor of 3 from the velocity of $c_0 = 176.6\,\mathrm{m/s}$ found

at equilibrium. The sound velocity then rises sharply, returning to the value c_0 at a density roughly 20% above the equilibrium density. Measurements at high frequencies (i.e., 5 MHz) reveal a much smaller dip in the lateral compression modulus and a sound velocity that is always materially larger than that at low frequencies and thus indicate the presence of significant dispersion [10, 11].

In Ref. [2], these features were exploited to suggest that the propagation of sound in these lipid mixtures can be described by the equation

$$\frac{\partial^2}{\partial\tau^2}\Delta\rho^A = \frac{\partial}{\partial z}\left[\left(c_0^2 + p\Delta\rho^A + q(\Delta\rho^A)^2\right)\frac{\partial}{\partial z}\Delta\rho^A\right] - h\frac{\partial^4}{\partial z^4}\Delta\rho^A \ . \quad (1)$$

Here, $\Delta\rho^A = \rho^A - \rho_0^A$ is the difference between the lateral mass density of the membrane and its empirical equilibrium value of $\rho_0^A = 4.035\times10^{-3}\,\mathrm{g/m^2}$, and the low frequency sound velocity is $c_0 = 176.6\,\mathrm{m/s}$. The coefficients p and q were fitted to measured values of the sound velocity as a function of density. Although high frequency sound velocity measurements indicate that the dispersive coefficient, h, must be positive, neither the magnitude of h nor the specific form of this term have been verified experimentally. In practice, the only role of h is to establish the linear size of solitons, and it can thus be chosen, e.g., so that the width of the soliton is comparable to that known for nerve pulses. Here, we choose to work with the dimensionless variables u, x and t defined as

$$u = \frac{\Delta\rho^A}{\rho_0^A} \quad x = \frac{c_0}{\sqrt{h}}z \quad t = \frac{c_0^2}{\sqrt{h}}\tau \ . \quad (2)$$

With this choice of variables, eq. (1) assumes the form

$$\frac{\partial^2 u}{\partial t^2} = \frac{\partial}{\partial x}\left(B(u)\frac{\partial u}{\partial x}\right) - \frac{\partial^4 u}{\partial x^4} \quad (3)$$

with

$$B(u) = 1 + B_1 u + B_2 u^2 \ . \quad (4)$$

The qualitative features of the empirical compression modulus require that $B_1 < 0$ and $B_2 > 0$. In the numerical work described below, we will adopt the parameter values $B_1 = -16.6$ and $B_2 = 79.5$ found in Ref. [2]. Eq. (3) can be recognized as a generalization of the Boussinesq equation, and it is known to have exponentially localized "solitonic" solutions which propagate without distortion for a finite range of sub-sonic velocities. We now determine the analytic form of these solitons.

Since we seek solutions which propagate without distortion, we regard u as a function of $\xi = x - \beta t$ and rewrite Eq. (3) as

$$\beta^2\frac{\partial^2 u}{\partial\xi^2} = \frac{\partial}{\partial\xi}\left(B(u)\frac{\partial u}{\partial\xi}\right) - \frac{\partial^4 u}{\partial\xi^4} \ . \quad (5)$$

We can integrate this equation twice with the assumption that u vanishes at spatially infinity to obtain

$$\frac{\partial^2 u}{\partial\xi^2} = (1-\beta^2)u + \frac{1}{2}B_1u^2 + \frac{1}{3}B_2u^3 \ . \quad (6)$$

It is clear from this equation that exponentially localized solutions are possible if $\beta^2 < 1$. Multiplication by $\partial u/\partial\xi$ and a final integration leave us with the result

$$\left(\frac{\partial u}{\partial\xi}\right)^2 = (1-\beta^2)u^2 + \frac{1}{3}B_1u^3 + \frac{1}{6}B_2u^4 \ . \quad (7)$$

It is clear that u is symmetric about its maximum value. The solution will grow from 0 until it reaches a maximum value at which $\partial u/\partial\xi = 0$. Equation (7) indicates that this is possible only if

$$1 > |\beta| > \beta_0 = \sqrt{1 - \frac{B_1^2}{6B_2}} \ . \quad (8)$$

For the parameters $B_1 = -16.6$ and $B_2 = 79.5$ adopted in [2], we find $\beta_0 \approx 0.649851$. We will use these parameter values in the remainder of this paper.

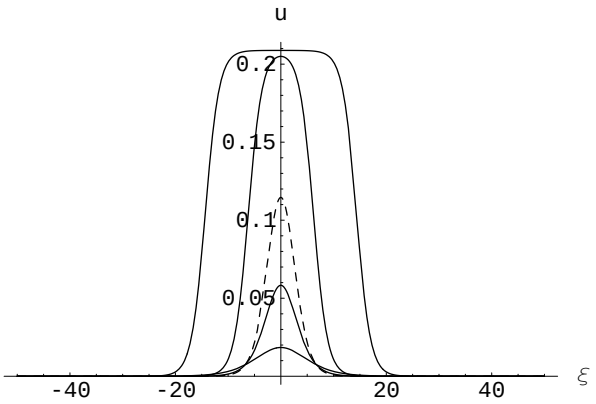

FIG. 1: Soliton profiles for velocities $\beta = \beta_0 + 4\times10^{-9}$, 0.65, 0.734761, 0.85, and 0.95. The maximum height diminishes as a function of β. The width of the soliton diverges for both $\beta \to \beta_0$ and $\beta \to 1$ and has a minimum at $\beta \approx 0.734761$, which corresponds to the dashed curve.

We thus expect localized solutions for $\beta_0 < |\beta| < 1$. When this condition is met, the right side of Eq. (7) will have two real roots, $u = a_\pm$ with

$$a_\pm = -\frac{B_1}{B_2}\left(1 \pm \sqrt{\frac{\beta^2-\beta_0^2}{1-\beta_0^2}}\right) \ . \quad (9)$$

It is readily verified that the desired solitonic solutions of Eq. (3) have the analytic form

$$u(\xi) = \frac{2a_+a_-}{(a_+ + a_-) + (a_+ - a_-)\cosh\left(\xi\sqrt{1-\beta^2}\right)} \ . \quad (10)$$

These solutions are shown in Figure 1 for a selection of soliton velocities.

As expected, Eq. (3) can be obtained from a suitable energy density. We thus seek an energy density, $\mathcal{E}$, such that Eq. (3) will result from variation of the corresponding Lagrangian density. To this end, it is useful to introduce the dimensionless displacement, $s(x,t)$, defined as $u = \partial s/\partial x$. The energy density can then be written as

$$\mathcal{E} = \frac{1}{2}\left(\frac{\partial s}{\partial t}\right)^2 + \left[\frac{1}{2}u^2 A(u) + \frac{1}{2}\left(\frac{\partial u}{\partial x}\right)^2\right] \tag{11}$$

with

$$A(u) = 1 + \frac{1}{3}B_1 u + \frac{1}{6}B_2 u^2 \ . \tag{12}$$

The two terms in Eq. (11) represent the kinetic and potential energy densities, respectively. The corresponding Lagrangian density is obtained by changing the sign of the potential energy term, and Eq. (1) follows by standard variational arguments. This form of the energy density leads to two important observations. First, we note that the energy density simplifies considerably if u describes a soliton and is given by Eq. (10). Specifically, use of the equation of motion allows us to write the energy density as $\mathcal{E}_{\rm sol} = u^2 A(u)$. The specific form of Eq. (10) is sufficiently simple that the energy of a soliton can be calculated analytically and involves only elementary functions.

It is also useful to consider the total energy associated with an arbitrary solution, $u(x,t)$, of Eq. (3) as given by the integral over all space of the energy density, $\mathcal{E}$, of Eq. (11). Recognizing perfect differentials when they arise and making use of the equation of motion, Eq. (3), we find the expected result that the energy is independent of time for an arbitrary choice of $u(x,t)$. (This result assumes either that $u(x,t)$ vanishes as $|x| \to \infty$ or that it satisfies periodic boundary conditions in x.) It is also useful to consider the time dependence of the the integral of u over all space,

$$U = \int u(x,t)\, dx \ . \tag{13}$$

It is clear from the equation of motion that $\partial^2 U/\partial t^2$ can be expressed as an integral of perfect differentials. Hence, $\partial^2 U/\partial t^2 = 0$ if u vanishes at spatial infinity or is periodic. Thus, the time dependence of U is elementary and can include only a constant term and a term linear in t. As we shall see below, U is independent of time when $u(x,t)$ is periodic.

NUMERICAL CONSIDERATIONS

We would like to investigate a number of questions associated with the stability of the solitons of Eq. (10). Although the simplicity of the analytic form of these solitons suggests that it may be possible to solve the problem of infinitesimal stability analytically, we have elected to consider this problem numerically. To this end, it is convenient to re-write Eq. (3) as two first-order equations. We obtain

$$\frac{\partial u}{\partial t} = \frac{\partial v}{\partial x} \ , \qquad \frac{\partial v}{\partial t} = \frac{\partial f}{\partial x} \tag{14}$$

with

$$f = u + \frac{1}{2}B_1 u + \frac{1}{3}B_2 u^2 - \frac{\partial w}{\partial x} \ , \tag{15}$$

where $w = \partial u/\partial x$ (and incidentally $v = \partial s/\partial t$). (Note that the first of Eqs. (14) ensures that the spatial integral of u is independent of time if v is chosen to be periodic.) Equations (14) are well-suited to numerical solution using a variant of the two-step Lax-Wendroff method [12]. We consider the function, $u(x,t)$, on a primary mesh of equally spaced points, $(p\Delta x, q\Delta t)$, where it has the values u_{pq}. (Evidently, we must demand $\Delta x < \beta \Delta t$ in order to satisfy the usual Courant condition, which is necessary but not sufficient to ensure numerical stability.) The mesh is then extended to include half-integer values of p and/or q. It is evident from Eqs. (14) and (15) that the functions u, v, and f live naturally on the points (p,q) and $(p+1/2, q+1/2)$ and that w lives naturally on the points $(p+1/2, q)$ and $(p, q+1/2)$.

The algorithm is implemented as follows: Establish the initial values of u and v on the points $(p,0)$. (If u is a solitonic solution, we simply have $v(x,0) = -\beta u(x,0)$.) At every time step, the values of $w_{p+1/2,q}$ are obtained as

$$w_{p+1/2,q} = \frac{u_{p+1,q} - u_{p,q}}{\Delta x} \ , \tag{16}$$

and these values can be used to construct f_{pq} using a similarly symmetric difference formula. One then proceeds to the evaluation of the functions u and v a time $\Delta t/2$ later. In proceeding from q to $q+1/2$, we define,

$$u_{p+1/2,q+1/2} = \frac{1}{2}\left(u_{p,q} + u_{p+1,q}\right) + \frac{\Delta t}{2\Delta x}\left(v_{p+1,q} - v_{p,q}\right) \ . \tag{17}$$

The values of $w_{p,q}$ and $f_{p+1/2,q+1/2}$ are obtained as in Eq. (16), and $v_{p+1/2,q+1/2}$ is obtained as in Eq. (17). A slightly different procedure is adopted in going from time $q+1/2$ to $q+1$. In this case,

$$u_{p,q+1} = u_{p,q} + \frac{\Delta x}{\Delta t}\left(v_{p+1/2,q+1/2} - v_{p-1/2,q+1/2}\right) \ , \tag{18}$$

the values of $w_{p+1/2,q+1}$ and $f_{p,q+1}$ are obtained as in Eq. (16), and $v_{p,q+1}$ is obtained in analogy with Eq. (15). This algorithm is both fast and stable in practice. (For the periodic boundary conditions and the choice of $\Delta x = 0.1$ and $\Delta t = 0.001$, used below, it was possible to follow 10^6 time steps without discernible loss of accuracy.)

It is useful to note that energy of Eq. (11) is not rigorously conserved by this numerical algorithm. In the following numerical examples, the energy was found to decrease at a roughly constant rate proportional to Δx^2. This fact was used to make an appropriate choice of $\Delta x = 0.1$. The corresponding value of $\Delta t = 0.001$ was selected to yield full numerical stability.

NUMERICAL RESULTS

Small amplitude noise

Our primary numerical concern is to study the stability of the solitonic solutions of Eq. (10) with respect to "infinitesimal" perturbations. We employ the parameters $B_1 = -16.6$ and $B_2 = 79.5$ adopted in [2], for which $\beta_0 \approx 0.650$. We will show results for an initial soliton with velocity $\beta = \beta_1 \approx 0.735$. This soliton has a width (i.e., full width at half maximum) of roughly 6.24, which is the minimum width possible for the values of B_1 and B_2 considered. There is, of course, no reason to believe that a soliton on a discrete lattice with finite Δx will have a profile identical to the analytic form of Eq. (10). The use of this analytic form in establishing the initial values of u and v thus inevitably introduces a measure of noise into the numerical system. Since there is no other "natural" choice for the initial form of the solitonic excitation, this noise represents the best approximation to infinitesimal perturbations that can be realized in a numerical study.

In an analytic approach to the question of infinitesimal stability, one considers the time evolution of the sum of the soliton under investigation and a small excitation, $\delta u(x,t) = \psi(x,t)$. The equation of motion (3) is then expanded to first order in ψ, and expressed in terms of t and $\xi = x - \beta t$,

$$\frac{\partial^2\psi}{\partial t^2} - 2\beta\frac{\partial^2\psi}{\partial t\partial\xi} + \beta^2\frac{\partial^2\psi}{\partial\xi^2} = \frac{\partial^2(B(u)\psi)}{\partial\xi^2} - \frac{\partial^4\psi}{\partial\xi^4}\,. \quad (19)$$

It follows that solutions to this (non-Hermitean) equation can be written as the product of functions $\psi_\lambda(\xi)$ and $\exp(\lambda t)$. If one or more of the resulting values of λ has a positive real part, the corresponding $\psi_\lambda(x,t)$ will grow exponentially with time, and the initial solitonic solution will be locally unstable. Since it is our aim to detect precisely such exponential stabilities (if present), it is of no consequence that the numerical noise introduced by the finite mesh size is small. Exponential instabilities will be apparent if they are present. The finite size of Δx also means that there is a smallest wave length perturbation which can be studied on the lattice. In practice, potential instabilities involving such wave lengths will be invisible to numerical studies only if they are orthogonal to those wave lengths which *can* be investigated reliably with the Δx chosen. While this is not impossible, it is unlikely.

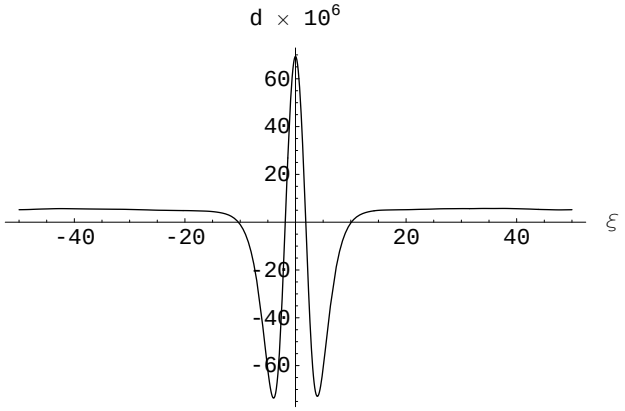

FIG. 2: The difference $d(\xi)$ between the time-averaged numerical soliton and the analytic soliton for the minimum width soliton with $\beta = \beta_1 \approx 0.735$. The average has been performed over 1000 units of time, during which the soliton travels more than 100 times its own width.

Results were obtained with $\Delta x = 0.1$ and $\Delta t = 0.001$. The spatial lattice was chosen to be periodic with length 100. For $\beta = \beta_1 \approx 0.735$, the exact energy of the soliton is 0.0377. The energy of this initial state is smaller by 1.5×10^{-6} when calculated on the lattice. Energy is not strictly conserved by the numerical algorithm adopted but rather decreases linearly with time over the time intervals considered. In the present case, energy is lost at the rate of 7.3×10^{-9} per unit time. We have followed this soliton for times as long as 1000 units, during which the soliton can propagate more than 100 times its own width. The energy loss is negligible, and there is absolutely no indication of instability. (Note that the discrepancy in the initial energy is proportional to Δx^2; the rate of energy loss scales like Δx^3.)

We can illustrate soliton stability in the following manner. We first determine the location of the maximum of the soliton as a function of time. The constancy of its velocity over large time intervals provides an initial indication of the stability of the soliton. In the present case, this velocity is found to be stable roughly 0.02% less than the initial velocity of the analytic soliton. (This error scales with Δx^2.) There are, of course, small fluctuations in the location of both the maximum density and, hence, the velocity due to the presence of noise. For the present example, such fluctuations in the location of the maximum are never greater than 0.004, which is 25 times smaller than Δx. (These fluctuations also scale like Δx^2.) Having identified the position of soliton as a function of time, each time frame is shifted to locate the soliton at a common point. A time-averaged soliton is then constructed in order to minimize the effects of noise. The difference between the time-averaged soliton and the analytic soliton is shown in Figure 2. The peak value of the time-averaged soliton is slightly (i.e., roughly 0.05%) higher than that of the analytic soliton, and it is

somewhat narrower than its analytic counterpart. (The size of these differences again scales with Δx^2.) This demonstrates the claim that the analytic solitons are not identical to solitons on a finite mesh. Further, the systematic discrepancy between these two solutions is the source of and has a magnitude comparable to that of the noise in the system.

We now consider the nature of the "lattice noise" in the system as a function of time by subtracting the time averaged soliton from the full $u(x,t)$ at each time update and constructing the root mean square of the resulting noise as a function of time. If the soliton is stable, the resulting rms noise should be bounded as a function of time. If the soliton were unstable, however, we would expect to find systematic differences in the vicinity of the soliton maximum which are well above noise level and which grow exponentially with time. The spatial distribution of noise at later times shows no sign of such systematic effects, and its magnitude is the same both near and far from the location of the soliton. The calculated rms noise is shown in Figure 3 as a function of time. Again, there is no sign of such instabilities. Since qualitatively similar results are found for other values of β, we conclude that the solitons of Eq. (3) are stable with respect to small perturbations.

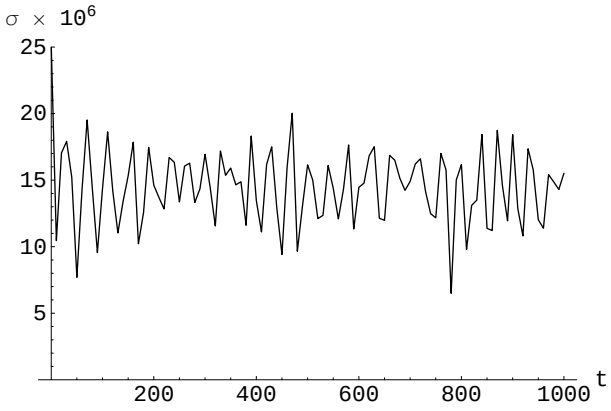

FIG. 3: Time evolution of rms noise level σ for the minimal width soliton over 1000 units of time.

It is also possible to study soliton stability in the presence of larger amplitude noise. This is most easily done by choosing a form of $u(x,0)$ which consists of both the (analytic) soliton of interest and a linear combination of the lowest $k \leq K$ periodic waves on the interval L, $a_k \sin(2\pi kx/L + \phi_k)$, with phases chosen at random and amplitudes chosen at random subject to a constraint on the overall rms noise level at $t = 0$. The analysis proceeds as above. We have considered the case of $K = 10$ with an initial rms noise as large as 5% of the maximum amplitude of the soliton. The results are similar to those found for small amplitude noise: There are no indications of soliton instability.

Soliton genesis

It is also instructive to consider finite-amplitude disturbances and to see how a localized but non-solitonic initial state evolves with time. To illustrate this, we choose $u(x,0)$ to be the minimum width soliton of Eq. (10). In this case, however, we distort the second initial condition and choose $v(x,0) = -p\,\beta u(x,0)$ with $p = 0.5$. Thus, the initial field is *not* solitonic. The time evolution shows that this initial pulse "sheds" matter and changes its shape through the emission of a smaller soliton, which moves in the opposite direction, and small amplitude waves, which run ahead of the solitons with velocity $\beta \approx 1$. The two solitons are captured in Figure 4 at $t = 50$. The velocity of the larger soliton is $\beta = 0.799$ and its maximum is at $x = 139.515$ whereas the smaller has $\beta = -0.948$ and maximum at $x = 52.871$. The shape of each of these solitons is accurately described using Eq. (10) with the corresponding measured velocity. These two solitons account for virtually all of the initial energy of the system; approximately 0.3% of this energy is associated with the small amplitude motion distinct from the solitons. In Figure 5 the two solitons have been subtracted out, and only the difference is plotted. This confirms that the shapes are indeed solitonic.

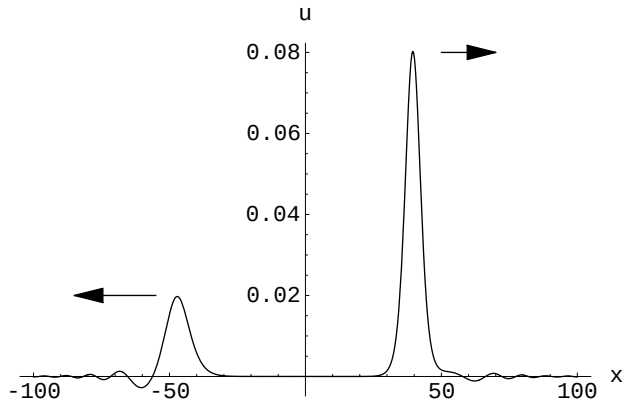

FIG. 4: A minimal width soliton with an initial velocity, β, 50% lower than the corresponding analytic value, shown at $t = 50$. It has divided into two solitons of different sizes, propagating in opposite directions. Small-amplitude waves run ahead of the solitons with velocity $\beta \approx 1$; the region between the solitons is essentially noise free. (See also Figure 5). Note that the length of the periodic lattice has been increased here to avoid interference effects between the solitons and the leading small amplitude waves.

Similar results have been obtained for other non-solitonic initial pulse forms (e.g., Gaussian pulses). In short, for the cases explored, non-solitonic initial excitations evolve into solitons and small amplitude non-solitonic disturbances. In infinite space, dispersion ensures that the solitonic and non-solitonic components will become spatially distinct and that the amplitude of the

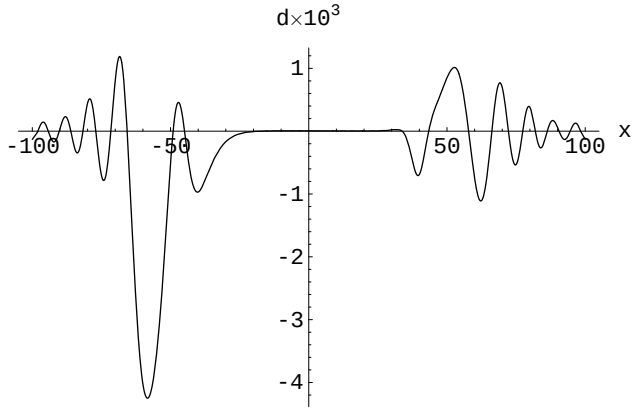

FIG. 5: The graph in Figure 4 with the two solitons subtracted out to leave only the small-amplitude waves running ahead of the solitons.

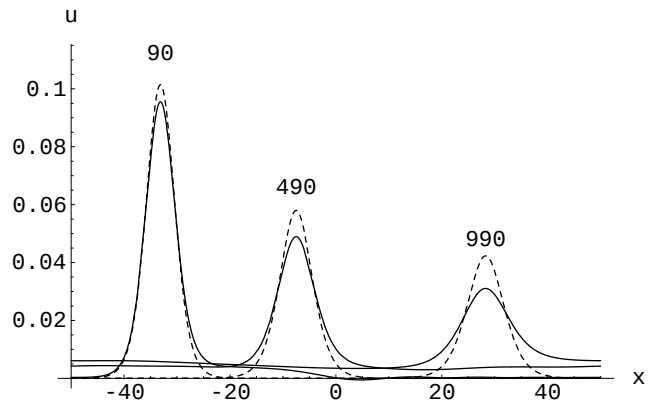

FIG. 6: Decaying soliton (fully drawn) with $\kappa = 0.05$, initially at $x = 0$. The dashed curves depict the analytic solitons with the instantaneous velocity of the numeric solitons. The numbers above the peaks indicate the running time, and their particular values have been chosen for illustrative purposes. The soliton has in fact wrapped around the periodic lattice more than 9 times during the time interval of the simulation.

latter will decrease with time. This is obviously not the case for the periodic lattice considered here.

Solitons and dissipation

It is also possible to consider the consequences of dissipation on soliton propagation. The inclusion of viscosity in the Navier-Stokes velocity results in an additional term on the right of Eq. (3) of the form $\kappa\partial^3 u/\partial x^2\partial t$. This term is readily incorporated in our numerical approach by the inclusion of the term $+\kappa\partial v/\partial\xi$ in Eq. (15). We have performed numerical studies with the value $\kappa = 0.05$. With this choice of κ, the height of the soliton is reduced by roughly 70% at $t = 990$, has travelled more than 100 times its initial width. As energy is dissipated, the soliton accelerates, and its profile changes with the expected drop in its amplitude. Over the entire time range considered, we find that the soliton profile is consistent with the analytic soliton profile of Eq. (10) appropriate for the corresponding instantaneous velocity of the pulse. This is illustrated in Figure 6, which shows the comparison of analytic solitons (in infinite space) and these numerical results including dissipation at several times.

For several reasons, this agreement is necessarily only approximate. First, some time is required for the soliton profile to adjust to the exact form corresponding to its instantaneous velocity. Obviously, only a limited time is available for this adjustment in the presence of dissipation. More importantly, the time-independence of the spatial integral of u is not affected by the inclusion of dissipation. Thus, $u(x,t)$ approaches a constant value for all x as $t \to \infty$. On a periodic lattice, as here, this constant is non-zero. This effect is clearly seen in Figure 6, and it is obviously not included in the analytic form of Eq. (10) valid in infinite space. Figure 6 shows no indication of the catastrophic break-up of the soliton into small amplitude waves which might be anticipated in the presence of strong dissipation. It should be noted that magnitude of the dissipation considered here is large compared to what is to be expected in biomembranes and nerves, where little or no change in pulse shape is observed over distances roughly 20 times than the pulse width.

CONCLUSIONS

We have considered here a number of tests of the stability of the solitons associated with the modified Boussinesq equation, Eq. (3). After finding the analytic form of these solitons, we turned to a numerical investigation (with periodic boundary conditions) of the their stability with respect to various perturbations. These solitons were found to be stable with respect to the "smallest possible" perturbations inevitably induced by the finite size of the numerical mesh and to finite but small periodic perturbations. Solitons are found to be produced by arbitrary localized but non-solitonic initial excitations. Finally, we have shown that solitons retain their characteristic properties even in the presence of relatively strong dissipation. It was argued in Ref. [2] that the measured compression modulus of lipids of biological membranes are suitable for the production of solitons.

These findings may be of immediate relevance for the propagation of the action potential in nerve axons [2]. The solitons described above are subject to friction and dissipation. Nerve membranes are not homogeneous, i.e., they vary both in thickness (e.g., at the site of the soma) and in the specific composition of lipids and proteins. Elastic constants may therefore vary locally. In the present paper we have shown that neither noise nor dissipation affect the propagation of solitary waves as such

but rather lead only to slight changes in amplitude and velocity. These pulses are therefore likely to be robust with respect to the unavoidable variance in shape and composition of biological membranes and to dissipative hydrodynamic processes which accompany the observed thickness changes in nerves [6]. Thus, the present results suggest that a model of nerve pulses as *stable* solitons is viable even in a realistic physiological environment and and that such a model may provide an immediate and reliable explanation of associated mechanical [6] and thermodynamic [3, 4, 5] effects that remain unexplained in the presently accepted Hodgkin-Huxley model [1].

We thank Hans Fogedby, Mogens Høgh Jensen, Bo-Sture Skagerstam, and Erwin Neher for valuable discussions.

[1] A. L. Hodgkin and A. F. Huxley, *A Quantitative Description of Membrane Current and its Application to Conduction and Excitation in Nerve*, J. Physiol. **117**, 500–544 (1952).

[2] T. Heimburg and A. D. Jackson, *On soliton propagation in biomembranes and nerves*, Proc. Natl. Acad. Sci. USA **102**, 9790-9795 (2005).

[3] B. C. Abbott, A. V. Hill and J. V. Howarth, *The positive and negative heat production associated with a nerve impulse*, Proc. R. Soc. London. B **148**, 149-187 (1958).

[4] J. V. Howarth, R.D. Keynes and J. M. Ritchie, *The origin of the initial heat associated with a single impulse in mammalian non-myelinated nerve fibres*, J. Physiol. **194**, 745–793 (1968).

[5] J. M. Ritchie and R. D. Keynes, *The production and absorption of heat associated with electrical activity in nerve and electric organ*, Quart. Rev. Biophys. **392**, 451–476 (1985).

[6] K. Iwasa and I. Tasaki, *Mechanical changes in squid giant-axons associated with production of action potentials*, Biochem. Biophys. Research Comm. **95**, 1328–1331 (1980).

[7] Y. Kobatake, I. Tasaki and A. Watanabe, *Phase transition in membrane with reference to nerve excitation*, Adv. Biophys. **2**, 1–31 (1971).

[8] J. H. Ipsen, G. Karlstrom, O. G. Mouritsen, H. Wennerstrom, and M .J. Zuckermann, *Phase equilibria in the phosphatidylcholine-cholesterol system*, Biochim. Biophys. Acta **905**, 162-172 (1987).

[9] T. Heimburg, *Mechanical aspects of membrane thermodynamics - estimation of mechanical properties of lipid membranes close to the chain melting transition*, Biochim. Biophys. Acta **1415**, 147-162 (1998).

[10] S. Halstenberg, T. Heimburg, T. Hianik, U. Kaatze, and R. Krivanek. *Cholesterol induced variations in the volume and enthalpy fluctuations of lipid bilayers*, Biophys. J. **75**, 264-271 (1998).

[11] W. Schrader, H.Ebel, P. Grabitz, E. Hanke, T. Heimburg, M. Höckel, M. Kahle, F. Wente, and U. Kaatze, *Compressibility of lipid mixtures studied by calorimetry and ultrasonic velocity measurements*, J. Phys. Chem. B **106**, 6581-6586 (2002).

[12] W. H. Press, S. A. Teukolsky, W. T Vetterling, and B. P. Flannery, *Numerical recipes in C (2nd edition,*Cambridge University Press (1994).